

ENERGY-SPECIFIC SOLAR RADIATION DATA FROM MSG: CURRENT STATUS OF THE HELIOSAT-3 PROJECT

Marion Schroedter-Homscheid⁽¹⁾, Jethro Betcke⁽²⁾, Gerhard Gesell⁽¹⁾,
Detlev Heinemann⁽²⁾ & Thomas Holzer-Popp⁽¹⁾

⁽¹⁾ Deutsches Zentrum für Luft- und Raumfahrt e. V. (DLR), Deutsches Fernerkundungsdatenzentrum (DFD),
Oberpfaffenhofen, D-82234 Wessling, Germany, phone: +49-8153-28 28 96, fax: +49-8153-28 1363,
e-mail: M.Schroedter-Homscheidt@dlr.de, Gerhard.Gesell@dlr.de, Thomas.Holzer-Popp@dlr.de

⁽²⁾ Universität Oldenburg, Abteilung Energie- und Halbleiterforschung, D-26129 Oldenburg,
e-mail: Jethro.Betcke@uni-oldenburg.de, Detlev.Heinemann@uni-oldenburg.de

ABSTRACT

HELIOSAT-3 aims at the operational quantification of surface solar irradiance in cloud free and cloudy situations and additional energy-specific parameters as direct normal irradiance, angular distribution of diffuse irradiance, illuminance, and photosynthetically active radiation (PAR) taking actual distributions of atmospheric absorbers and scatterers into account. The new method relies on input information on physical cloud properties (e.g. optical depth), aerosol optical depth and type, water vapour concentration and ozone distribution which are derived from MSG or ERS-2/ENVISAT measurements. First MSG-based results for the clear sky case will be shown.

MSG-SEVIRI based cloud and water vapour level 2 and level 3 products are given as examples. Additionally, ERS-2 and ENVISAT data is used to derive aerosol optical depth and type as well as ozone concentration. Recent improvements of the aerosol retrieval method SYNAER and a 5 degree climatology data set for the MSG field of view based on 1997/1998 ERS-2 data are presented.

1. INTRODUCTION

Solar energy technologies such as photovoltaics, solar thermal power plants, passive solar heating/cooling systems and daylighting in buildings are expected to continue their rapid growth.

Another emerging market is forecasting the electricity load and production for electric utilities. Scheduling of large power plants needs a precise knowledge of the load. Besides temperature, irradiance is the major environmental influence on the electricity demand.

The availability of reliable solar radiation data is of high value for planning and operating of solar energy systems and as basis data set for electricity load forecasting. Both long term time series and near real time data is needed. In detail global, diffuse and direct irradiance have to be separated.

A detailed assessment of solar irradiance requires not only knowledge on the distribution of clouds, but also information on aerosol load, total water vapour content and ozone concentration in the atmosphere. Radiative

transfer models together with fast parameterisations are used to derive surface irradiance separated in direct and diffuse components.

In the following sections a MSG-SEVIRI-based cloud parameter retrieval, a SEVIRI-based total water vapour column retrieval, an ERS-2 based aerosol climatological data set and ENVISAT based ozone information are presented. The last section deals with first results using such parameters to derive direct and diffuse irradiance together with a first validation.

2. SEVIRI CLOUD RETRIEVAL

The AVHRR Processing scheme Over cLOUDs Land and Ocean (APOLLO, [1], [2], [3], [4]) was the first AVHRR data processing scheme to make use of all five spectral channels during daytime. It discretises all pixels into four different groups called cloud-free, fully cloudy, partially cloudy (i.e. neither cloud-free nor fully cloudy) and snow/ice-contaminated, before deriving physical properties.

Within APOLLO, clouds are categorised into three layers according to their top temperature. The layer boundaries are set to 700 hPa and 400 hPa. The associated temperatures are derived from standard atmospheres. Further, each fully cloudy pixel is checked to see whether it is thick or thin cloud, depending on its 11 μm and 12 μm brightness temperatures and, during daytime, its channel 0.6 μm and 0.8 μm reflectances. Thin clouds (with no thick clouds underneath) are taken as ice clouds, i.e. cirrus, whereas thick clouds are treated as water clouds.

Cloud cover is derived for each cloud type separately. To derive the fractional cloud cover of the partially cloudy pixels at daytime, the relationship of the measured 0.6 μm and 0.8 μm reflectances to the mean of the fully cloudy and cloud-free reflectances in a local neighbourhood (e.g. 50 by 50 pixels) is used. More details of these methods are given in [1].

At daytime, for each fully cloudy pixel, clouds optical depth, liquid/ice water path and IR-emissivity are derived by means of parameterisation schemes using the reflectance at 0.6 μm . The parameterisation scheme is based on the directional hemispherical cloud top

reflectance, which is obtained from the (measured) bi-directional top of atmosphere reflectance by applying an anisotropy correction, correction due to ozone absorption and subtracting the surface part of the reflectance transmitted through the cloud. Details of the method can be found in [2].

The adaptation of APOLLO to MSG-SEVIRI caused some changes:

- Defaults of thresholds for most of the APOLLO algorithms have to be set depending on the region covered by the data to be processed. The thresholds itself are either set explicitly or are dynamically derived from local histogram calculations in neighbourhood-boxes. Therefore, all explicitly set thresholds and default settings have been changed, i.e. their values have been adapted to the regions visible by SEVIRI (especially necessary for non-European areas). These presets must be physically reasonable, i.e. are climatologically or empirically determined for the complete SEVIRI view and usually depend on region and season.
- Step 2 and 3 in the APOLLO processing contain corrections for regional peculiarities, e.g. cold currents and thermal fronts in the ocean, deserts with frequent sand storms etc. These local peculiarities can cause misclassifications and wrong values for the cloud parameters and the processing must correct for it. These corrections depend not just on the region with the certain peculiarity but also on the degree of experience with it. Therefore, each APOLLO processing scheme is specific for the region it is applied to and APOLLO/SEV and APOLLO/AVH differ here as much as the AVHRR-view (covering mainly Europe due to field-of-view of DLRs receiving system at Oberpfaffenhofen) and SEVIRI-view are different.

A check if results of APOLLO/SEV are reasonable, has been done by means of comparisons of typical cloud parameter values derived from both, SEVIRI and AVHRR, and by means of a quality analysis based on many years of experiences with APOLLO/AVH.

3. SEVIRI TOTAL WATER VAPOUR COLUMN RETRIEVAL

Several retrieval methods to derive total water vapour content (TWC) over land from MSG SEVIRI data have been tested. The Thermodynamic Initial Guess Retrieval (TIGR, [7]) data set was used to represent possible atmospheric states of temperature and humidity distribution. The TIGR data set was developed at the Laboratoire de Meteorologie Dynamique (LMD, Paris) especially for the development of retrieval methods. It includes more

than 2300 radiosonde profiles from all over the world. The following steps were performed:

- a) all TIGR humidity profiles were integrated vertically to calculate 'true' TWC
- b) forward radiative transfer calculations (MODTRAN3.7, [8] and [9]) were performed with all TIGR temperature and humidity profiles to simulate MSG satellite measurements in the 10.8 and 12 μm channels
- c) retrieval algorithms were applied to this simulated MSG radiances in order to derive TWC
- d) TWC column derived from these simulated MSG radiances were compared with the values calculated directly from the TIGR profiles

A 'split window' retrieval algorithm for the retrieval of water vapour column over land as published by Kleespies and McMillan ([10], [6]) was tested. The method uses the split window channels at 10.8 and 12 μm . In general, infrared measurements are affected by air temperature, surface temperature, surface emissivity, water vapour and absorption of other atmospheric gases. 'Split window' channels are selected close to each other, so that equal emissivity and absorption of other gases than water vapour can be assumed. Surface temperature is the same for both channels as this parameter is not dependent of the observer's wavelength. This reduces the dependence of measurements in these channels to air temperature and water vapour absorption. Two situations with varying surface temperatures are selected and therefore, two brightness temperature measurements can be exploited. Having these two equations the air temperature dependence can be eliminated. MSG offers the possibility to use this approach as it measures in a 15 minutes temporal resolution and therefore, can deliver 'two situations with varying surface temperatures' during the daily temperature cycle.

Eq. 1 describes the functional relationship between brightness temperatures and TWC.

$$\frac{\tau_{11}}{\tau_{12}} = \frac{(T_{11}^A - T_{11}^B)}{(T_{12}^A - T_{12}^B)}$$

$$TWC = fct \left\{ \frac{1}{\sec \theta} \ln \left(\frac{\tau_{11}}{\tau_{12}} \right) \right\} \quad (1)$$

T is the brightness temperature in channel 11 or 12 μm , θ is the satellite zenith angle, A and B are two temporal different situations and τ stands for transmission. A minimum difference of 8 K between T_{12} in situation A and B is required to avoid noise effects.

Kleespies and McMillin proposed a linear relationship between the transmission ratio term and TWC. Testing the whole TIGR data set it turned out that a third order

polynomial describes the relationship better. Assumably, the reasons for this non-linear behaviour are (a) non-neglectable absorption of other atmospheric gases if TWC is very small and (b) saturation of absorption lines for large TWC values.

A significant dependence on satellite zenith angle was found. Especially for larger TWC values a simple cosine airmass correction as used in Eq.1 is not suitable anymore. An explicit calculation of airmass correction in the infrared needs detailed information about the temperature profile of the atmosphere. Unfortunately, this will not be available later in the operational processing scheme. Therefore, a parameterisation was developed. All coefficients of the third order polynomial can be parameterised with sufficient accuracy using a quadratic fit.

Fig. 1 gives TWC for March 17th, 2004 for a subset from line 2783 to 3248 and element 600 to 3000. Please note, that the method derives TWC only over land which is most relevant for solar energy applications. Further data gaps are due to cloud cover.

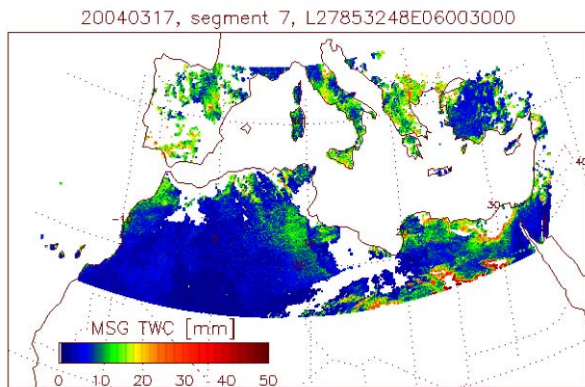


Fig. 1: MSG derived TWC in mm, March 17th, 2004

Fig. 2 shows an example of the level 3 total water vapour column product. This product is generated in a 3-step-approach: (1) average all level 2 data available in a 0.5x0.5° latitude/longitude grid box, (2) interpolate empty boxes locally, and (3) fill still empty boxes with a background climatology based on the NASA Water Vapor Project (NVAP) data set http://eosweb.larc.nasa.gov/PRODOCS/nvap/table_nvap.html.

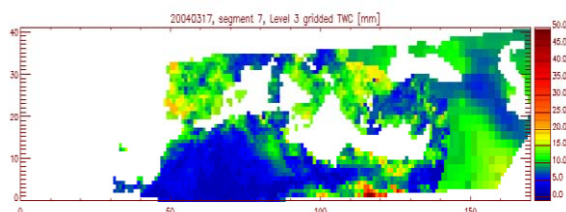


Fig. 2: Level 3 water vapour column product [mm] for March 17th, 2004 for 26.75 - 47.25° N, -33.75° - 51.75° E

4. ERS-2 AEROSOL DATA SET

A synergetic aerosol retrieval method (SYNAER), which exploits a spectrometer radiometer combination to retrieve aerosol optical thickness and type, has been developed with GOME (Global Ozone Monitoring Instrument) and ATSR-2 (Along Track Scanning Radiometer), both onboard the European Radar Satellite ERS-2 ([11], [12]). The methodology selects the most plausible type of aerosols from remote sensing observations in each pixel without relying on any background data set.

It is the goal to produce (and in future update) a satellite based aerosol climatology for the observation area of MSG. For this purpose the SYNAER method will be implemented and work operationally with the sensors SCIAMACHY (Scanning Imaging Absorption Spectrometer for Atmospheric Cartography) and AATSR (Advanced ATSR) onboard ENVISAT. As a backup climatology 14 months of data in 1997/1998 from GOME and ATSR-2 over the MSG area were evaluated. Due to GOME operations such data is available only for 3 days each month. It describes annual average optical thickness values of major components (sulfate/nitrate, soot, dust, sea salt) of the atmospheric aerosol load. The final aim is to deliver 4 seasonal climatology data sets with a 1 degree horizontal grid. Due to cloud coverage and method inherent limitations this one year data set was obtained as first product for a 5 degree grid.

A first validation of the method and recent investigations in the community have led to the definition of promising improvements in the aerosol model: Absorption features of soot and mineral components as well as the vertical profile of dust outbreak events require updating. A reprocessing of the climatology data set is under way. Further details on methodology and generation of this data set is given in a paper by Holzer-Popp et al., [13].

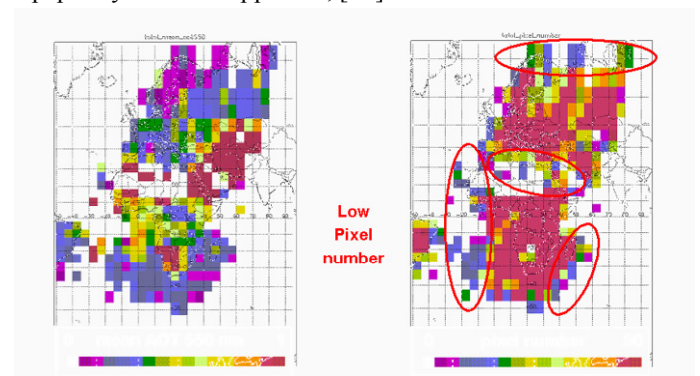


Fig. 3: 14 months GOME/ATSR-2 aerosol climatology. Mean AOT is given on the left, pixel number used on the right. Areas with a small pixel number are marked. Despite of the small data base the aerosol distribution is rather smooth with a mean aerosol optical thickness

of 0.26 and some interesting features can already be observed (Fig. 3): Largest optical thickness values above 1 occur over / near the desert areas, whereas the Scandinavian area or oceanic zones far off from the continents show lowest values. Also biomass burning plumes from South America and Central Southern Africa are indicated over the Atlantic.

Fig. 4 shows also the component-wise mean aerosol optical thickness maps: Sulfate/nitrate aerosols which are included in all modelled aerosol types as background contribution show even clearer the unpolluted oceanic and Northern areas. Soot occurs most prominently over industrialised/densely populated areas in Central/Eastern Europe as well as over biomass burning source areas in Central/Southern Africa and in their plumes over the ocean (Fig. 4). Dust is dominant around desertic areas (Sahara, Namib, Near East). Sea salt occurs with low values also at inland locations which indicates to the limits of separating this component with low impact on the total optical thickness, but it should be noted that its maximum occurs over the Southern Atlantic. Some areas are not covered by the basic data set because of either too high cloudiness or too bright surface.

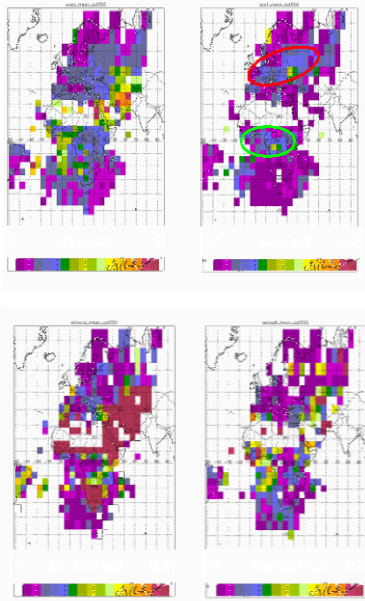


Fig. 4: GOME/ATSR-2 aerosol climatology separated for watersoluble aerosols, soot, mineral dust and sea salt. Industrial areas and biomass burning areas can clearly be identified in the soot component.

5. ENVISAT-BASED OZONE

Ozone total column data is provided by SCIAMACHY onboard ENVISAT. SCIAMACHY is a spectrometer measuring atmospheric absorption in spectral bands from the ultraviolet to the near infrared (240 nm - 2380 nm). From these observations total column amounts and stratospheric profiles of a multitude of atmospheric

constituents are retrieved on a global scale [14]. Currently, SCIAMACHY data of V5.04 is available.

Due to the scanning geometry of SCIAMACHY total column ozone observations are heterogeneously distributed in time and space. To gain synoptic distributions of total column ozone considering atmospheric variability the SCIAMACHY observations are sequentially assimilated into a 3D Chemistry Transport Model, describing all relevant chemical and physical processes [15] [16].

The 3D global chemical-transport-model DLR-ROSE 3.0 is used. It is based on the ROSE model described in detail in [17] and [18], but was significantly improved. The model covers all relevant gas-phase stratospheric chemical processes. Heterogeneous processes are also included in the model. It accounts for about 100 reactions, including oxygen, hydrogen, carbon, nitrogen chlorine, and bromine species. The basic chemical time-step is 15 min. All species are transported every 90 minutes using a Lin and Rood scheme. The model is driven by wind- and temperature fields of the European Center for Medium Range Weather Forecast (ECMWF). The spatial discretisation of the DLR-ROSE 3.0 uses a $2.8^\circ \times 2.5^\circ$ lon.-lat. spherical grid and 43 log-pressure levels between 0 and 56 km altitude (316. to 0.316 hPa) resulting in a vertical step size of 1.3 km. Globally gridded 3D fields are available every 6 hours.

6. SEVIRI IRRADIANCE RETRIEVAL

Overview

The existing Heliosat-1 method ([19],[20], and [21]) determines the global horizontal irradiance from data of the Meteosat 7 visible channel with an accuracy of approx. 22 % for hourly values in North-Western Europe. The extended infrared channels of the SEVIRI instrument, the higher spatial and temporal resolution of the visible channel of Meteosat 8 and the availability of ENVISAT data allow for the development of a more accurate method: A clear sky module, that determines the irradiance in the absence of clouds, and a cloud module that uses the clear sky irradiance and cloud information as input.

SOLIS clear sky module

In the Heliosat-1 method the clear sky irradiance is determined with an empirical model that uses climatological values of the Linke turbidity factor as input. The new SOLIS clear sky module [22] uses a more physical approach. The radiative transfer model LibRadtran [23] is used to calculate direct and diffuse in each of the Kato correlated-k wavelength bands, for the solar zenith angles 0° and 60° . Water vapour, aerosol and ozone information are used as input. Currently, these data are taken from a climatology. In

the near future data will be used from the MSG SEVERI instrument and ENVISAT (see section 2 - 5).

The direct clear sky irradiance for a complete day is than obtained by fitting the modified Lambert-Beer function on the two points calculated with Libradtran:

$$I^i(\Theta_z) = I_{ext}^i \exp\left(-\frac{\tau_0}{\cos^\alpha(\Theta_z)}\right) \cos(\Theta_z) \quad (2)$$

Where, I^i is the direct irradiance for waveband i , I_{ext}^i is the extraterrestrial irradiance for waveband i , Θ_z is the solar zenith angle, α is a fitting parameter, and τ_0 is the optical depth which is also used as a fitting parameter. For the calculation of the diffuse irradiance the factor $\cos(\Theta_z)$ is left out. This approach saves considerable calculation time without a significant loss of accuracy compared to a complete use of the radiative transfer model.

Cloudy sky model

In the Heliosat-1 method the global irradiance under cloudy conditions is obtained by multiplying the global clear sky irradiance with the clear sky index which is obtained by means of an empirical method from the Meteosat 7 visible channel. Due to the modular approach this method can be combined with the results of the SOLIS clear sky module. In its existing form this would mean the loss of the spectral information produced by SOLIS. Therefore a separate weighting function has been developed to account for the influence of clouds on the spectral irradiance.

A completely new cloudy sky module, based on the cloud information provided by the APOLLO scheme is currently under development. It is divided into two parts for overcast situations and for broken cloud situations, respectively. The overcast part is based on a parameterisation that uses cloud optical depths and the effective cloud-particle radii as input. For the latter currently an average value is used. However, implementation of the Nakajima scheme [24] is foreseen. The broken cloud part will be based on the cloud characteristics provided by APOLLO.

Direct and Diffuse Irradiance

In the Heliosat-1 model the global horizontal irradiance is split in a diffuse and a direct part by applying the Skartveith-Olsen model [25]. This model was adapted to make better use of the SOLIS output.

Validation and Implementation

As a first step the intrinsic accuracy of the SOLIS clear sky module was investigated separately by applying it only to cloudless days. For this particular test the atmospheric data input was retrieved from ground measurements. RMSE values of 2.3% and 4.0% were

found for direct irradiance and global horizontal irradiance, respectively.

In a second step the SOLIS clearsky module was combined with the Heliosat-1 cloudy sky module to obtain data for all-weather situations. Meteosat 7 data and climatological atmospheric data were used as input. The resulting global horizontal irradiance did not differ significantly from the data obtained with the Heliosat-1 procedure. However, the RMSE of the direct and diffuse irradiance was reduced by appr. 2%.

The first step towards implementation with MSG data was made by adapting the existing Heliosat-1 method for the use of MSG data. A first validation showed a reduction in the RMSE of 1 to 2%, that can be ascribed to the higher temporal resolution of MSG (Fig. 5).

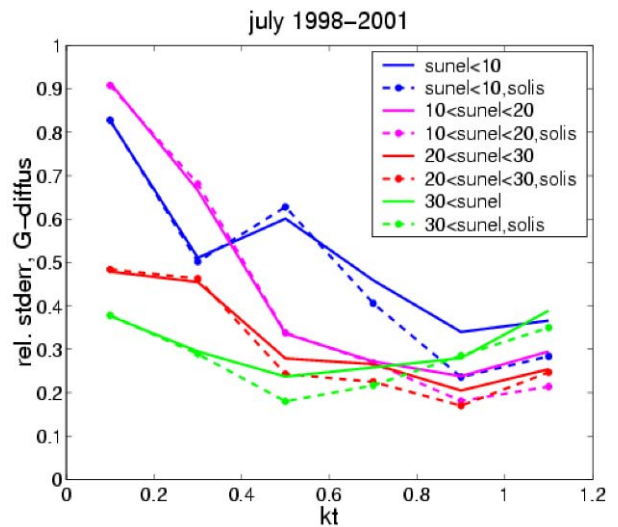


Fig. 5: Reduction in the r.m.s error in the diffuse irradiance of SOLIS (dashed line) compared with Heliosat-1 (solid line) for different solar elevations as a function of clear sky index.

The combination of the SOLIS clear sky module with the Heliosat-1 cloud module with MSG data as input is currently under investigation. Implementation and validation of SOLIS clear sky in combination with the new cloud module is planned for the end of the year.

7. CONCLUSIONS

A method to derive solar surface irradiance separated both into direct and diffuse parts is under development in the HELIOSAT-3 project. The clear sky case has been successfully investigated and validated. Especially, improvements in the retrieval of diffuse irradiance were found. To improve available input data sets the following steps have been taken: (1) The APOLLO scheme to derive cloud optical properties has been successfully adapted to MSG-SEVIRI data. (2) A method to derive daily total water vapour content over land from MSG-SEVIRI has been developed and validated. (3) An aerosol background climatology has

been generated from ERS-2 data from 1997/1998 using the SYNAER retrieval method. In parallel SYNAER is adapted to ENVISAT data currently. (4) ENVISAT-based daily global ozone data fields are made available as additional input.

Further steps are the development of the cloudy case irradiance retrieval scheme and the full integration of all four input data sources into the operational HELIOSAT-3 scheme. The HELIOSAT-3 scheme is intended to run on the full MSG disk in a full pixel resolution.

Acknowledgements

ERS-2 data was received via the ERS AO project SENECA (AO id 106) and first MSG test data sets were received via the MSG AO project HELIOSAT-3 (AO id 105). The HELIOSAT-3 project is funded by the EC (NNK5-CT-200-00322).

8. REFERENCES

1. Saunders R.W. and K.T. Kriebel: An improved method for detecting clear sky and cloudy radiances from AVHRR data. *Int. J. Rem. Sens.*, 9, 123-150,1988
2. Kriebel, K.T., R.W. Saunders and G. Gesell: Optical Properties of Clouds Derived from Fully Cloudy AVHRR Pixels. *Beiträge zur Physik der Atmosphäre*, Vol. 62, No. 3, pp. 165-171, 1989
3. Gesell G.: An Algorithm for Snow and Ice Detection Using AVHRR Data: An Extension to the APOLLO Software Package. *International Journal of Remote Sensing*, Vol. 10, Nos. 4 and 5, pp. 897-905,1989
4. Kriebel K. T., Gesell G., Kästner M., Mannstein H., The cloud analysis tool APOLLO: Improvements and Validation, *Int. J. Rem. Sens.*, 24, 2389-2408, 2003
5. Saunders R.W.: Cloud top temperature /height: A high resolution imagery product from AVHRR data, *Meteorological Magazine*,117, 211-221,1988
6. Kleespies J.T. & L.M. McMillin: Retrieval of precipitable water from observations in the Split Window over varying surface temperatures, *J. Appl. Met.*, 29,851-862., 1990
7. Chedin A., et al., The improved initialisation method: a high resolution physical methods for temperature retrievals from satellites of the TIROS-N series, *J. Appl. Met.*, 24,128-143, 1985
8. Abreu L.W. & G.P. Anderson (Hrsg.): *The MODTRAN 2/3 Report and LOWTRAN 7 MODEL*.-Philips Laboratory, Hanscom, 1996
9. Berk A., et al., *MODTRAN4 User's Manual*, Airforce Research Laboratory, Hanscom., <http://www.cis.rit.edu/~dirtsig/doc>, 1999
10. Kleespies, J.T. & L.M. McMillin, Physical retrieval of precipitable water using the Split Window technique, *Conference on Satellite Meteorology, Remote Sensing and Applications*, S. 55-57,1984
11. Holzer-Popp, T., M. Schroedter, and G., Gesell, Retrieving aerosol optical depth and type in the boundary layer over land and ocean from simultaneous GOME spectrometer and ATSR-2 radiometer measurements, part I. *J. Geophys. Res.*, 107, D21, pp. AAC16-1 – AAC16-17, 2002
12. Holzer-Popp, T., M. Schroedter, and G., Gesell, Retrieving aerosol optical depth and type in the boundary layer over land and ocean from simultaneous GOME spectrometer and ATSR-2 radiometer measurements, part II, *J. Geophys. Res.*, 107, D24, pp. AAC10-1 – AAC10-8, 2002
13. T. Holzer-Popp, M. Schroedter-Homscheidt, Synergetic aerosol retrieval from ENVISAT, *ENVISAT/ERS Symposium*, Salzburg, 6.-10.9.2004
14. *DLR: ENVISAT-1 SCIAMACHY Level 1c to 2 NRT and Off-line Processing Algorithm Description*, ENV-ATB-SAO-SCI-2200-0003, Issue 2, December, 2000
15. Erbertseder, T., et al.: Assimilation of ENVISAT products for continuous monitoring of atmospheric trace gases - First results from EVIVA, submitted to *ESA ERS/ENVISAT Symposium 2004*
16. Erbertseder T., F. Baier, M. Bittner, Hildenbrand, B: Global Ozone Analyses by assimilating SCIAMACHY observations into a 3D CTM, *EGS-AGU-EGU Assembly*, Nice, 2003
17. Rose K. and Brasseur G.: A three-dimensional model of chemically active trace species in the middle atmosphere during disturbed winter conditions, *J. Geophys. Res.*, 94, 16387-16403, 1989
18. Riese M., Tie X., Brasseur G., and Offermann D.: Three-dimensional simulation of stratospheric trace gas distributions measured by CRISTA, *J. Geophys. Res.*, 104, 16419-16435, 1999
19. Cano D., Monget J., Albuissou M., Guillard H., Regas N., Wald L., A method for the determination of the global solar radiation from meteorological satellite data, *Solar Energy*, 37, 31-39,1986
20. Beyer H., et al., Mod-ifications of the heliosat procedure for irradiance estimates from satellite images, *Solar Energy*, 56, 207-212,1996
21. Hammer A., *Anwendungsspezifische Solarstrahlungsinformationen aus Meteosat-Daten*, PhD, School of Mathematics and Natural Sciences, University of Oldenburg, 2000
22. R.W. Mueller et al, Rethinking satellite-based solar irradiancemodelling, The SOLIS clear sky module, *Rem. Sens. Environ.*, 91,160-174, 2004
23. B. Mayer et al., Systematic long term comparison of spectral UV measurements and UVSPEC modelling results, *J. Geophys. Res.*, 102, 8755-8767, 1997
24. T. Nakajima and M. King, Determination of the optical thickness and effective particle radius of clouds from reflected solar radiation measurements, *Journal of the Atmospheric Sciences*, 47., 1878-1893,1990
25. Skartveit et al., A hourly diffuse fraction model with correction for variability and surface albedo, *Solar Energy*, 63, 173-183,1998